

Synthesis of Potassium Niobate (KNbO₃) Thin Films by Low-Temperature Hydrothermal Epitaxy

Wojciech L. Suchanek

Sawyer Research Products, Inc., 35400 Lakeland Boulevard, Eastlake, Ohio 44095

Received October 3, 2003. Revised Manuscript Received January 9, 2004

Orthorhombic KNbO₃ thin films were deposited on SrTiO₃ (100) and LiTaO₃ (001) substrates by low-temperature hydrothermal epitaxy at 180–210 °C using aqueous solutions containing Nb₂O₅ and KOH. The films were thoroughly characterized by X-ray diffraction, Rutherford backscattering, and scanning electron microscopy. The KNbO₃ films were uniformly distributed on the entire substrate area, exhibited high stoichiometry, and did not show evidence of interdiffusion or chemical reaction at the film/substrate interface. Their microstructures were determined by the substrate used, the synthesis temperature, and the concentration of the reactants. The KNbO₃ films on SrTiO₃ (100) substrates with thickness of 45 nm to 1.28 μm were smooth and transparent, with microstructures strongly suggesting single crystal growth mechanism. They were pure orthorhombic phase with (011) orientation and probably single-domain. Conversely, the KNbO₃ films with higher thickness (>3.5 μm) exhibited very rough microstructure with textured columnar grains. Such films were also orthorhombic but with mixed (100)/(011) orientation. This work demonstrated for the first time deposition of heteroepitaxial KNbO₃ films on single-crystal substrates using low-temperature hydrothermal epitaxy in a well-defined range of synthesis conditions. The low synthesis temperatures, which are below the 225 °C phase transition temperature of KNbO₃, resulted in formation of films that appear to exhibit improved features as compared to the films prepared by high-temperature processing.

Introduction

Potassium niobate (KNbO₃) is a very promising material for surface acoustic wave (SAW) devices and high-performance bulk-wave transducers.¹ The electromechanical coupling coefficient (k^2) of the surface wave in a single-crystal KNbO₃ can be as high as 53%, which is one order of magnitude larger than that of LiNbO₃.² The bandwidth is about 20% and insertion losses are 2–6 dB.² The acoustic wave velocities in KNbO₃ are 3500–7500 m/s³ and the temperature coefficient of frequency (TCF) ranges between 0 and 170 ppm/K depending upon crystallographic orientation.² The KNbO₃ exhibits large piezoelectric nonlinearity. The 45° rotated Y-cut X-propagated KNbO₃ has 25 dB larger efficiency than Y–Z LiNbO₃; thus the KNbO₃ single crystal is considered as a promising material for SAW elastic convolvers with super high efficiency and process gain.⁴ In addition to excellent piezoelectric properties, the KNbO₃ has a large electrooptic coefficient, high nonlinear optical coefficient, and excellent photorefractive characteristics⁵ that make it a very promising candidate for optical applications such as optical waveguides, frequency doublers,⁶ intensity modulators,⁷

optical switching and modifiable interconnections,⁷ and holographic storage systems.⁸

Unfortunately, KNbO₃ melts incongruently and crystallizes cubic perovskite-type structure, which undergoes two phase transformations during cooling: cubic to tetragonal at 435 °C and tetragonal to orthorhombic at 225 °C.⁶ This behavior makes it very difficult to obtain large, crack-free, single-domain crystals. For these reasons, KNbO₃ films have been investigated on a variety of substrates as very promising candidates for both optical and frequency control applications. KNbO₃ thin films offer several advantages over bulk single crystals of the same material, such as improved compositional control and the ability to utilize low growth rates,⁹ in addition to being cheaper and more easily obtainable on low-cost commercial substrates.¹⁰ For electrooptic applications, thin films of KNbO₃ feature lower driving voltages and higher modulation speeds than bulk single crystals; moreover, they have the potential for monolithic integration.¹¹ For SHG applications of optical waveguides, utilization of KNbO₃ thin films is preferable over bulk single crystals because of the high cost of KNbO₃ large single crystals and

(1) Yamanouchi, K.; Odagawa, H.; Kojima, T.; Onoe, A.; Yoshida, A.; Chikuma, K. *Electron. Lett.* **1998**, *34*, 702.

(2) Yamanouchi, K.; Odagawa, H. *IEEE Trans. Ultrason., Ferroelectrics, Frequency Control* **1999**, *46*, 700.

(3) Zaitsev, B. D.; Kuznetsova, I. E.; Borodina, I. A.; Joshi, S. G. *Ultrasonics* **2001**, *39*, 51.

(4) Cho, Y.; Oota, N.; Odagawa, H.; Yamanouchi, K. *J. Appl. Phys.* **2000**, *87*, 3457.

(5) Wu, X.; Looser, H.; Wuest, H.; Arend, H. *J. Cryst. Growth* **1986**, *78*, 431.

(6) Fukuda, T.; Uematsu, Y. *Jpn. J. Appl. Phys.* **1972**, *11*, 163.

(7) Kip, D. *Appl. Phys. B* **1998**, *67*, 131.

(8) Wang, J. Y.; Guan, Q. C.; Wei, J. Q.; Wang, M.; Liu, Y. G. *J. Cryst. Growth* **1992**, *116*, 27.

(9) Graettinger, T. M.; Rou, S. H.; Ameen, M. S.; Auciello, O.; Kingon, A. I. *Appl. Phys. Lett.* **1991**, *58*, 1964.

(10) Beckers, L.; Buchal, C.; Fluck, D.; Pliska, T.; Gunter, P. *Mater. Sci. Eng. A* **1998**, *253*, 292.

(11) Hoerman, B. H.; Nichols, B. M.; Nystrom, M. J.; Wessels, B. W. *Appl. Phys. Lett.* **1999**, *75*, 2707.

technological difficulties in forming in them waveguides by ion implantation, diffusion, or ion exchange.¹² The main factors for pursuing thin films in acoustic wave applications are a general miniaturization trend in electronic devices using SAW and BAW elements,¹³ and the task of SAW suppliers is to integrate as many external functions as possible into the SAW components.¹⁴ Another important factor in realizing the thin films approach is a possibility of enhancing almost all properties of SAW or BAW devices by designing appropriate film/substrate materials or even multilayered thin film structures. Subsequently, all essential properties can be tailored in wide ranges by using different combinations of materials, crystallographic orientations (cuts), and microstructures.¹⁵

So far, KNbO₃ thin films can be synthesized by the following methods: metalorganic chemical vapor deposition (MOCVD),^{16–19} pulsed-laser deposition,^{10,20–25} sputtering,^{26,27} liquid-phase epitaxy,^{28–30} and sol-gel.^{31–33} All these synthesis routes share similar disadvantages of high-temperature processing, requiring temperatures ranging between 600 °C and over 900 °C to obtain a crystalline KNbO₃ phase. The high synthesis temperatures cause typical problems such as difficulties to control potassium stoichiometry due to high volatilization of potassium oxide, interdiffusion between film and the substrate,^{20,21,24} formation of interphase layers (particularly in the case of using MgO substrate),^{21,24} and multidomain formation during cooling to room temperature.^{16,20–23,27,29,30} The presence of pyrochlore and/or amorphous phases, as well as porosity, was

reported particularly for the KNbO₃ films synthesized by the sol-gel method.^{32,33} In addition, liquid-phase epitaxy (LPE) is not well suited for films with thickness under 1 μm.³⁰

In other words, all previously used methods to synthesize KNbO₃ films yielded films with more or less deteriorated properties due to the high synthesis temperatures. Therefore, development of a low-temperature fabrication of KNbO₃ thin films, particularly at temperatures lower than the tetragonal to orthorhombic phase transformation of 225 °C appears to be necessary in order to realize multiple potential applications of the KNbO₃ films. Low-temperature hydrothermal techniques offer such possibilities. Several reports on low-temperature (30–285 °C) hydrothermal synthesis of KNbO₃ powders appeared recently in the literature,^{34–38} indicating potential for hydrothermal synthesis of KNbO₃ thin films. Several attempts to grow thin films of KNbO₃ or related compounds by the hydrothermal techniques were also reported. Komatsu et al. unsuccessfully attempted homoepitaxial growth of KNbO₃ on a multidomain KNbO₃ single crystal with polished pseudocubic {100} planes.³⁷ The deposit from the surface of the KNbO₃ single crystal was identified by X-ray diffraction as a mixture of an amorphous phase and orthorhombic KNbO₃ crystals with random orientation. The coating had multiple cracks and did not provide complete surface coverage.³⁷ Wu et al.^{39,40} reported hydrothermal-electrochemical synthesis of thin films of a related material, K₂Ta₂O₆, with a pyrochlore structure. The pyrochlore K₂Ta₂O₆ films were polycrystalline with a random orientation. However, no perovskite KTaO₃ phase could be obtained under these conditions.^{39,40} Lange et al. reported synthesis of epitaxial KTaO₃ films by low-temperature hydrothermal epitaxy at 175 °C.⁴¹

The objective of this work was to synthesize orthorhombic KNbO₃ films with a single crystallographic orientation and hopefully also single-domain, on such single-crystal substrates as SrTiO₃ (100) and LiTaO₃ (001) by hydrothermal epitaxy at about 200 °C, i.e., below the phase-transition temperature of 225 °C. The technique used was the low-temperature hydrothermal epitaxy developed originally by Lange,⁴² which was successfully applied to synthesize other epitaxial oxide films, such as BaTiO₃,⁴³ PbTiO₃,⁴⁴ and PZT,^{45–47} etc.

(12) Chow, A. F.; Lichtenwalner, D. J.; Auciello, O.; Kingon, A. I.; Busch, J. R.; Wood, V. E. *J. Appl. Phys.* **1995**, *78*, 435.

(13) Su, Q.-X.; Kirby, P.; Komuro, E.; Imura, M.; Zhang, Q.; Whatmore, R. *IEEE Trans. Microwave Theory Tech.* **2001**, *49*, 769.

(14) Meier, H.; Baier, T.; Riha, G. *IEEE Trans. Microwave Theory Tech.* **2001**, *49*, 743.

(15) Hickernell, F. S. *Int. J. High Speed Electron. Syst.* **2000**, *10*, 603.

(16) Nystrom, M. J.; Wessels, B. W.; Chen, J.; Marks, T. J. *Appl. Phys. Lett.* **1996**, *68*, 761.

(17) Onoe, A.; Yoshida, A.; Chikuma, K. *Appl. Phys. Lett.* **1996**, *69*, 167.

(18) Onoe, A.; Yoshida, A.; Chikuma, K. *Appl. Phys. Lett.* **2001**, *78*, 49.

(19) Chattopadhyay, S.; Nichols, B. M.; Hwang, J. H.; Mason, T. O.; Wessels, B. W. *J. Mater. Res.* **2002**, *17*, 275.

(20) Hung, L. S.; Bosworth, L. A. *Appl. Phys. Lett.* **1993**, *62*, 2625.

(21) Zaldo, C.; Gill, D. S.; Eason, R. W.; Mendiola, J.; Chandler, P. *J. Appl. Phys. Lett.* **1994**, *65*, 502.

(22) Gopalan, V.; Raj, R. *J. Am. Ceram. Soc.* **1995**, *78*, 1825.

(23) Christen, H. M.; Boatner, L. A.; Budai, J. D.; Chisholm, M. F.; Gea, L. A.; Marrero, P. J.; Norton, D. P. *Appl. Phys. Lett.* **1996**, *68*, 1488.

(24) Martin, M. J.; Alfonso, J. E.; Mendiola, J.; Zaldo, C.; Gill, D. S.; Eason, R. W.; Chandler, P. *J. Mater. Res.* **1997**, *12*, 2699.

(25) Zhang, D. M.; Li, Z. H.; Zhang, M. J.; Wang, X. D.; Huang, M. T.; Yu, B. M.; Xu, D. S.; Wang, Y. M. *Am. Ceram. Soc. Bull.* **2001**, *80*, 57.

(26) Thöny, S. S.; Lehmann, H. W.; Gunter, P. *Appl. Phys. Lett.* **1992**, *61*, 373.

(27) Chow, A. F.; Lichtenwalner, D. J.; Woolcott, R. R.; Graettinger, T. M.; Auciello, O.; Kingon, A. I.; Boatner, L. A.; Parikh, N. R. *Appl. Phys. Lett.* **1994**, *65*, 1073.

(28) Khachatryan, O. A.; Madayan, R. S. *Cryst. Res. Technol.* **1984**, *19*, 461.

(29) Hulliger, J.; Gutman, R.; Wuest, H. *J. Cryst. Growth* **1993**, *128*, 897.

(30) Gutmann, R.; Hulliger, J.; Reusser, E. *J. Cryst. Growth* **1993**, *126*, 578.

(31) Nazeri-Eshghi, A.; Kuang, A. X.; Mackenzie, J. D. *J. Mater. Sci.* **1990**, *25*, 3333.

(32) Nazeri, A.; Kahn, M. *J. Am. Ceram. Soc.* **1992**, *75*, 2125.

(33) Derderian, G. J.; Barrie, J. D.; Aitchison, K. A.; Adams, P. M.; McCartney, M. L. *J. Am. Ceram. Soc.* **1994**, *77*, 820.

(34) Lu, C. H.; Lo, S. Y.; Lin, H. C. *Mater. Lett.* **1998**, *34*, 172.

(35) Feng, S.; Li, G.; Li, L.; Li, X. *Rev. High Pressure Sci. Technol.* **1998**, *7*, 1362.

(36) Uchida, S.; Inoue, Y.; Fujishiro, Y.; Sato, T. *J. Mater. Sci.* **1998**, *33*, 5125.

(37) Komatsu, R.; Adachi, K.; Ikeda, K. *Jpn. J. Appl. Phys., Part 1* **2001**, *40*, 5657.

(38) Goh, G. K. L.; Lange, F. F.; Haile, S. M.; Levi, C. G. *J. Mater. Res.* **2003**, *18*, 338.

(39) Wu, Z. B.; Tsukada, T.; Yoshimura, M. *J. Mater. Sci.* **2000**, *35*, 2833.

(40) Wu, Z. B.; Tsukada, T.; Yoshimura, M. *J. Mater. Res.* **2000**, *15*, 1154.

(41) Goh, G. K. L.; Levi, C. G.; Lange, F. F. *J. Mater. Res.* **2002**, *17*, 2852.

(42) Lange, F. F. *Science* **1996**, *273*, 903.

(43) Chien, A. T.; Speck, J. S.; Lange, F. F.; Daykin, A. C.; Levi, C. G. *J. Mater. Res.* **1995**, *10*, 1784.

(44) Chien, A. T.; Sachleben, J.; Kim, J. H.; Speck, J. S.; Lange, F. F. *J. Mater. Res.* **1999**, *14*, 3303.

(45) Chien, A. T.; Speck, J. S.; Lange, F. F. *J. Mater. Res.* **1997**, *12*, 1176.

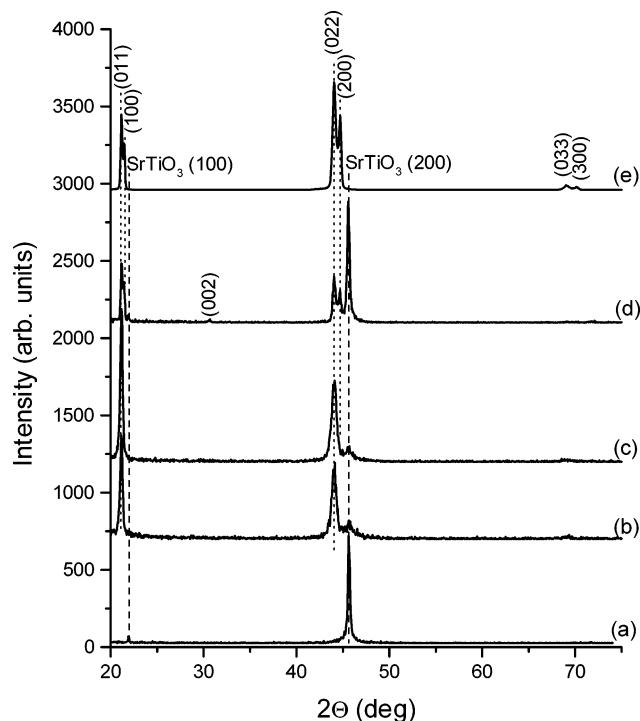


Figure 1. XRD patterns of orthorhombic KNbO_3 films deposited hydrothermally on single-crystal SrTiO_3 (100) substrates at 200 °C (48 h) from aqueous solutions containing (a) 4.0 m KOH and 0.50 m Nb_2O_5 ; (b) 6.0 m KOH and 0.50 m Nb_2O_5 ; (c) 6.0 m KOH and 0.20 m Nb_2O_5 ; (d) 10.0 m KOH and 0.05 m Nb_2O_5 ; and (e) 10.0 m KOH and 0.50 m Nb_2O_5 . Note absence of any deposits in (a), preferred (011) orientation of the KNbO_3 films in (b) and (c), and mixed (100)/(011) orientation of the KNbO_3 films in (d) and (e).

Experimental Procedure

Hydrothermal Synthesis of KNbO_3 Films. Niobium pentoxide (Nb_2O_5 , purity 99.9%, Alfa Aesar, Ward Hill, MA) and potassium hydroxide (KOH, pellets, assay 85 wt %, Fisher Scientific, Pittsburgh, PA) were used to prepare precursors for hydrothermal synthesis of KNbO_3 films. The concentration of the reactants in the aqueous precursors ranged between 0.05 and 0.50 m for Nb_2O_5 , and 2.0 and 14.0 m for KOH. It should be noted that all concentrations are expressed in molality (m), i.e. number of mols per 1 kg of H_2O . The KNbO_3 precursors were prepared in 100-mL PTFE bottles with screw caps, according to the following procedure. First, 6.60–46.20 g of KOH was fully dissolved in such quantities of de-ionized water to yield a total water content of 35–50 g. Following complete dissolution of the KOH in water, 0.465–6.645 g of Nb_2O_5 powders were added, as required by stoichiometry. Subsequently, the substrates, ultrasonicated earlier in isopropyl alcohol (assay min. 99%, histology grade, EM Science, Gibbstown, NJ) for 30 min and dried in air, were placed in the upper part of each bottle (below the solution level) using PTFE tubing as holders. The following single-crystal substrates were used in the hydrothermal experiments: (i) polished SrTiO_3 with (100) orientation (dimensions 5 mm × 5 mm × 0.5 mm, Coating and Crystal Technology, Inc., Kittanning, PA); (ii) polished SrTiO_3 (100) 1-in. wafers (Marketch International, Port Townsend, WA); and (iii) polished LiTaO_3 (001) (\approx 5–10 mm × 5–10 mm × 0.4 mm pieces from a broken 3-in. wafer, Sawyer Crystal Systems, Inc., Conroe, TX).

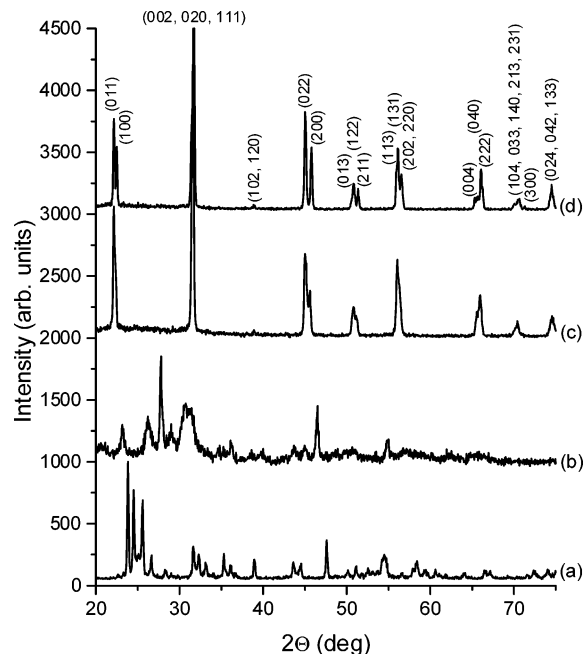


Figure 2. XRD patterns of the solid phases precipitated under hydrothermal conditions at 200 °C (48 h) simultaneously with the film deposition in the bulk of aqueous solutions with various chemical compositions: (a) no treatment; (b) 2.0 m KOH and 0.50 m Nb_2O_5 ; (c) 6.0 m KOH and 0.05 m Nb_2O_5 ; and (d) 10.0 m KOH and 0.50 m Nb_2O_5 . The observed phases were: (a) Nb_2O_5 (unreacted powder); (b) $\text{K}_4\text{Nb}_6\text{O}_{17}$ (major phase); (c) and (d) orthorhombic KNbO_3 .

The hydrothermal syntheses of KNbO_3 thin films were performed in autoclaves with a 13-in. internal diameter and internal length of 120 in. (manufactured by Autoclave Engineers, Erie, PA). In each experiment, 9–15 PTFE bottles containing the precursors and substrates were attached to a steel rack using steel wires. The PTFE bottles were closed tight using the screw caps, but all had capillary holes drilled through the caps (from the side) in order to allow pressure equilibration between the inside of the bottles and the internal parts of the autoclave. The rack with the attached PTFE bottles was placed inside the autoclave on a spacer, in such a way that it was positioned in the upper half of the autoclave. The bottom part of the autoclave was filled with de-ionized water to about half of the height of the spacer ($1/4$ of the autoclave volume). The autoclave was closed with a plug and three internal thermocouples were placed inside in order to measure temperatures in the upper and lower part of the rack with the bottles, as well as in the bottom section of the autoclave.

Most of the hydrothermal runs were carried out at the temperatures of 180 °C (48 h) or 200 °C (48 h). A very limited number of experiments was carried out also at 210 °C (48 h). The average measured heating rate in the temperature range of 20–210 °C was 0.48 °C/min. The corresponding pressures were the saturated vapor pressures of water at 180, 200, and 210 °C, i.e., 1.00, 1.55, and 1.91 MPa, respectively. The samples were cooled together with the autoclaves in an uncontrolled fashion.

After each synthesis run and opening the autoclave, the PTFE bottles with samples were removed from the rack. The solutions with precipitates (if any) were collected and stored for future reference. Some of the precipitates were washed several times with de-ionized water and subsequently dried. The films deposited on the substrates were removed from the holders, placed in glass beakers and subjected to ultrasonic cleaning in de-ionized water for 20 min and subsequently in isopropyl alcohol for 10 min. The substrates with films were dried overnight at room temperature.

Characterization of the Materials. Phase composition and crystallographic orientation of all synthesized films and selected powder precipitates was characterized by X-ray dif-

(46) Suchanek, W. L.; Oledzka, M.; Mikulka-Bolen, K.; Pfeffer, R. L.; Lencka, M.; McCandlish, L.; Riman, R. E. *Proceedings of Fifth International Conference on Solvothermal Reactions (ICSTR)*, East Brunswick, New Jersey, July 22–26, 2002; 2002; p 159.

(47) Oledzka, M.; Lencka, M. M.; Pinceloup, P.; Mikulka-Bolen, K.; McCandlish, L. E.; Riman, R. E. *Chem. Mater.* **2003**, *15*, 1090.

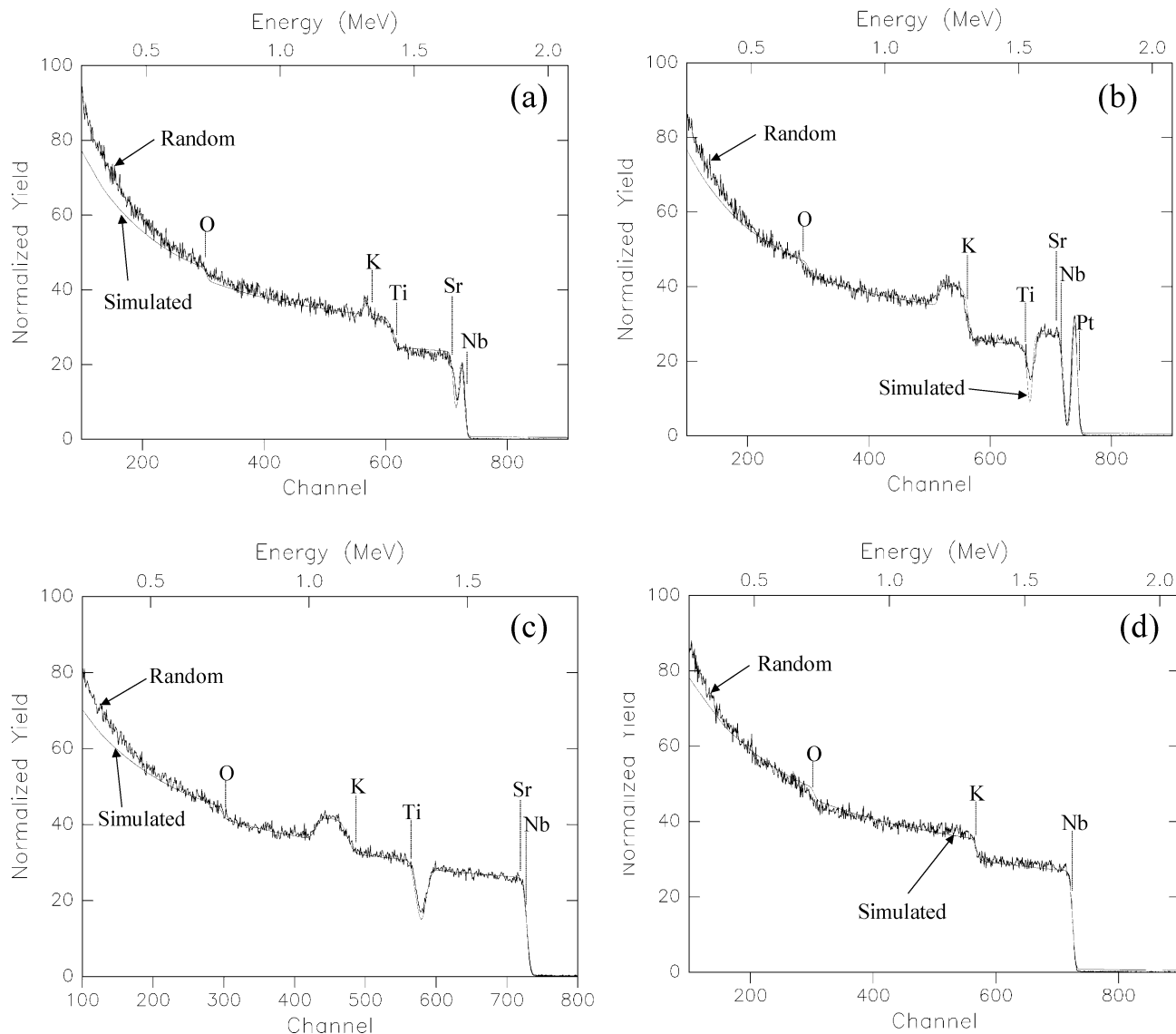


Figure 3. Random and simulated RBS spectra of typical KNbO_3 films deposited hydrothermally on single-crystal SrTiO_3 (100) substrates at 200 °C (48 h) from aqueous solutions containing: (a) 4.0 m KOH and 0.05 m Nb_2O_5 ; (b) 6.0 m KOH and 0.20 m Nb_2O_5 ; (c) 6.0 m KOH and 0.20 m Nb_2O_5 (coated twice); and (d) 10.0 m KOH and 0.50 m Nb_2O_5 . Thickness of the films was (a) 45 nm; (b) 270 nm; (c) 725 nm; and (d) over 3.5 μm . In (b) the first sharp peak is derived from a 6-nm-thick palladium layer which was sputtered on the film surface.

fraction using an Advanced Diffraction System X1 diffractometer (XRD, Scintag Inc.) using $\text{Cu K}\alpha$ radiation, in the 2θ range between 20 and 75° with a 0.05° step size and 0.3–0.7-s count time. The chemical identity and orientation of the materials was determined by comparing the experimental XRD patterns to standards compiled by the Joint Committee on Powder Diffraction and Standards (JCPDS), i.e., card 35-0734 for SrTiO_3 , 29-0836 for LiTaO_3 , 71-0946 for orthorhombic KNbO_3 , 08-0212 for cubic KNbO_3 , 28-0788 for $\text{K}_2\text{Nb}_6\text{O}_{16}$, and 21-1295 for $\text{K}_4\text{Nb}_6\text{O}_{17}$.

Chemical composition and thickness of selected films were measured by Rutherford backscattering (RBS). For this purpose, the film samples were attached to the stage of a goniometer in the beamline of a 1.7-MV tandem pelletron accelerator (model 5SDH, National Electrostatics Corporation, Middletown, WI). The 2.00-MeV He^{2+} ion beam was used to obtain the RBS spectra. The beam was collimated to a rectangular spot approximately 1 mm \times 1 mm. The RBS data were recorded over 800 channels. Compositional and thickness analysis of the films were done by matching the data to simulation spectra generated with the RUMP RBS analysis software package.^{48,49} To estimate the degree of crystalline order, selected samples were measured using ion channeling. This involved measuring the yield of backscattered ions (in

an energy window corresponding to backscattering events just beneath the films' surface) as a function of rotation angle. The resulting angular scan showed sharp dips in the yield at angles characteristic of crystalline plane directions. Subsequently, RBS spectra in the entire energy range were recorded in the channels with minimum yields and compared to the random spectra.

The morphology of selected synthesized KNbO_3 films was examined using scanning electron microscopy (SEM, model S-4500, Hitachi, Japan) at 5-kV accelerating voltage. The KNbO_3 films on the substrates were mounted directly to the metal sample holders using a conductive carbon tape. All film samples were sputtered with thin conductive layers of platinum prior to the SEM examination.

Results

Hydrothermal Deposition of KNbO_3 Films on SrTiO_3 (100) Substrates. A wide range of orthorhombic KNbO_3 films was synthesized under hydrothermal

(48) Doolittle, L. R. *Nucl. Inst. Methods* **1985**, *B9*, 334.

(49) Doolittle, L. R. *Nucl. Inst. Methods* **1986**, *B15*, 227.

conditions on SrTiO₃ (100) substrates during the course of this work. Typical XRD patterns of the deposited films are shown in Figure 1. No other XRD peaks except for those derived from either SrTiO₃ or KNbO₃ phases were detected. The films prepared at lower concentrations of KOH, which ranged between 4.0 and 6.0 m, were single-phase KNbO₃ with (011) orientation. Only the (011) and (022) reflections were visible in the XRD patterns (Figure 1b and c), in addition to the (100) and (200) reflections from the SrTiO₃ substrate (Figure 1a). At the KOH concentrations above 6.0 m, the films exhibited mixed (100)/(011) orientation, as demonstrated by presence of both (100), (200), (300), and (011), (022), (033), XRD peaks (Figure 1d and e). Orientation of the KNbO₃ films appeared to be independent of the Nb₂O₅ concentration in the investigated 0.05–0.50 m range.

Simultaneously with the film deposition, white solid precipitates were formed in almost all solutions of aqueous precursors used for the KNbO₃ films synthesis. At KOH concentration of 2.0 m only K₄Nb₆O₁₇ phase was detected by XRD (Figure 2b). At higher KOH concentrations, only the orthorhombic KNbO₃ phase crystallized in the bulk of the coating solutions (Figure 2c and d).

The synthesized KNbO₃ films had thicknesses ranging between 45 nm and >3.5 μm, as measured by the RBS technique. The RBS spectra confirmed high purity and stoichiometry of the deposited KNbO₃ films. Figure 3 shows RBS spectra representative of orthorhombic KNbO₃ films, with different thicknesses and crystallographic orientations. An RBS spectrum of a 45-nm-thick KNbO₃ film with (011) orientation is shown in Figure 3a. Figure 3b and c show RBS spectra of (011) oriented KNbO₃ films with thicknesses of 270 and 725 nm, respectively. A typical RBS spectrum of a thick (>3.5 μm) KNbO₃ film with a mixed (100)/(011) orientation is presented in Figure 3d. The recorded random RBS spectra were in a very good agreement with the calculated ones, indicating stoichiometric KNbO₃ composition and high purity of the films. They did not indicate any significant interdiffusion between the KNbO₃ films and the SrTiO₃ substrates.

Epitaxial relationship between the SrTiO₃ (100) substrate and the hydrothermally synthesized KNbO₃ (011) films has been demonstrated by the RBS ion channeling measurements. RBS ion channeling measurements of selected KNbO₃ (011) films indicated very high level of the film orientation. A proper angle for axial channeling could be calculated from angular scans, and an RBS spectrum was measured with the sample aligned at those angles. For typical KNbO₃ (011) films, comparison of the aligned ion channeling and random RBS spectra (Figure 4) shows that the films exhibit a very high level of orientation and are highly aligned with respect to the SrTiO₃ (100) substrate.

Microstructures of the KNbO₃ films further confirmed their high level of 3D orientation. Figure 5 shows representative microstructures of the KNbO₃ films. KNbO₃ (011) films with thickness ranging between 45 nm and 1.28 μm exhibited microstructures without clearly defined grains or grain boundaries (Figure 5a–c). They consisted of multiple layers of small building blocks (10-nm size), which often formed quasi-dendritic/fractal-like structures. Conversely, the films with the

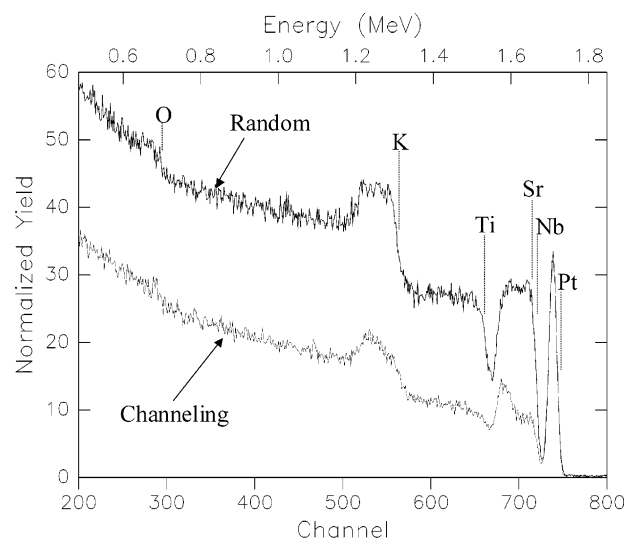


Figure 4. Random and ion channeling RBS spectra of the KNbO₃ (011) film deposited hydrothermally on single-crystal SrTiO₃ (100) substrates at 200 °C (48 h) from aqueous solutions containing 6.0 m KOH and 0.20 m Nb₂O₅. The first sharp peak with the same intensity in both RBS spectra is derived from a 6-nm-thick palladium layer which was sputtered on the film surface.

thickness of several μm were very rough and consisted of highly textured columnar grains, as shown in Figure 5d.

In most cases, the synthesized KNbO₃ films were very uniformly distributed on the SrTiO₃ substrates, including 1-in. wafers, and covered the entire substrate surface. All KNbO₃ films with 45 nm to 1.28 μm thickness were optically transparent irrespective of the orientation, whereas the KNbO₃ films thicker than 3.5 μm were milky and translucent. Neither cracks nor peeling-off were observed in the synthesized KNbO₃ films, except for a few samples with the highest film thickness (>3.5 μm). Occasionally, inclusions of KNbO₃ particles were incorporated in the films synthesized at 200–210 °C.

Hydrothermal Deposition of KNbO₃ Films on LiTaO₃ Substrates. KNbO₃ films were successfully deposited on LiTaO₃ (001) wafers at 180–200 °C at high KOH concentrations between 10 and 14 m. Typical XRD patterns of the KNbO₃ films on LiTaO₃ are shown in Figure 6. Some of the films appear to be orthorhombic with (100) orientation, as shown in Figure 6c. XRD patterns of other films indicate either KNbO₃ polycrystalline films with random orientation and possible cubic symmetry or formation of multidomain orthorhombic KNbO₃ having domains with different crystallographic orientations (Figure 6b).

Microstructure of a selected KNbO₃ film on LiTaO₃ substrate is shown in Figure 7. The film microstructure appears to be polycrystalline but with a high level of orientation. It is worth mentioning that a very few shallow etch pits were observed on the LiTaO₃ substrates during the deposition of KNbO₃ films.

Discussion

Regions of deposition of the KNbO₃ films on both SrTiO₃ and LiTaO₃ substrates as functions of the temperature, in the 180–200 °C range, and reactants'

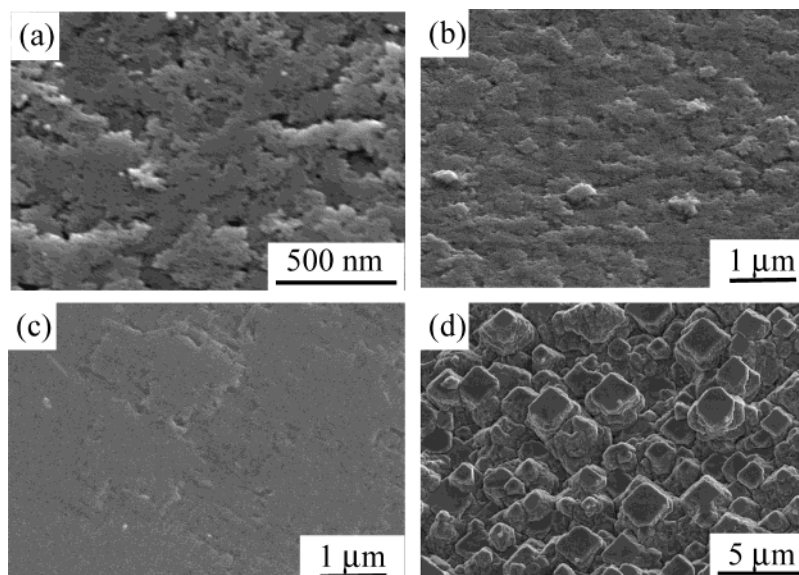


Figure 5. SEM photographs of orthorhombic KNbO_3 films deposited hydrothermally on single-crystal SrTiO_3 (100) substrates from aqueous solutions containing (a) 6.0 m KOH and 0.50 m Nb_2O_5 (200 °C, 48 h); (b) 6.0 m KOH and 0.20 m Nb_2O_5 (200 °C, 48 h); (c) 6.0 m KOH and 0.20 m Nb_2O_5 (210 °C, 48 h); (d) 10.0 m KOH and 0.50 m Nb_2O_5 (200 °C, 48 h).

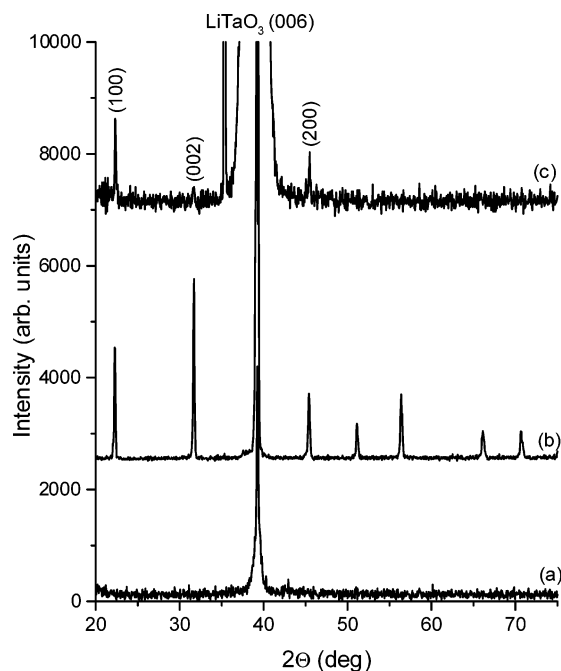


Figure 6. XRD patterns of KNbO_3 films deposited hydrothermally on single-crystal LiTaO_3 (001) substrates at 180 °C (a and c) and 200 °C (b) for 48 h from aqueous solutions containing (a) 6.0 m KOH and 0.20 m Nb_2O_5 (no film deposition); (b) 14.0 m KOH and 0.20 m Nb_2O_5 ; and (c) 10.0 m KOH and 0.20 m Nb_2O_5 .

concentrations are summarized in Figure 8. In general, higher KOH concentrations favored formation of the KNbO_3 films. The boundaries of the stability regions of the KNbO_3 films were around 5 m KOH at 200 °C and 7–9 m KOH at 180 °C. In addition, at the boundary KOH concentrations, the KNbO_3 films started forming at very low Nb_2O_5 concentration, whereas at higher Nb_2O_5 concentrations no deposition of any kind was observed. Because of the very limited number of synthesis experiments conducted at 210 °C, stability regions of the KNbO_3 films at this temperature were not established.

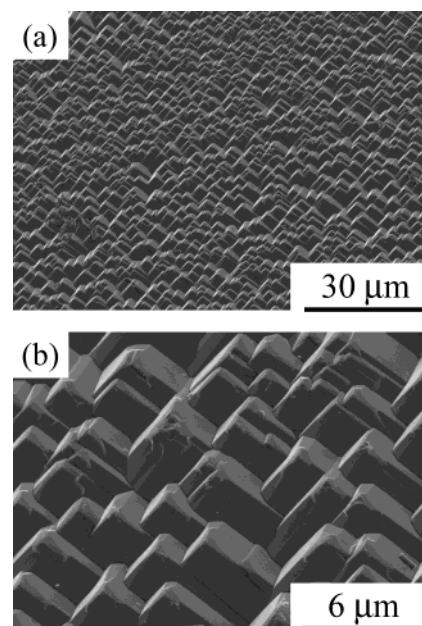


Figure 7. SEM photographs of a KNbO_3 film deposited hydrothermally on single-crystal LiTaO_3 (001) substrate at 180 °C (48 h); reactants concentration: 10.0 m KOH and 0.20 m Nb_2O_5 .

Although no attempts to grow orthorhombic KNbO_3 films below 180 °C were undertaken in this work, it is quite possible that the films could be deposited under such conditions. However, the films deposited at 180 °C, particularly those which were synthesized at lower concentrations of the reactants, tend to be much thinner than the corresponding films synthesized at 200 °C. Therefore, it seems that even if the deposition of orthorhombic KNbO_3 films were possible at temperatures lower than 180 °C, it would probably require rather high KOH and Nb_2O_5 concentrations with a possibility of producing very thin films and/or incomplete substrate coverage.

The morphology of the KNbO_3 films deposited on SrTiO_3 substrates was found to be a function of the KOH

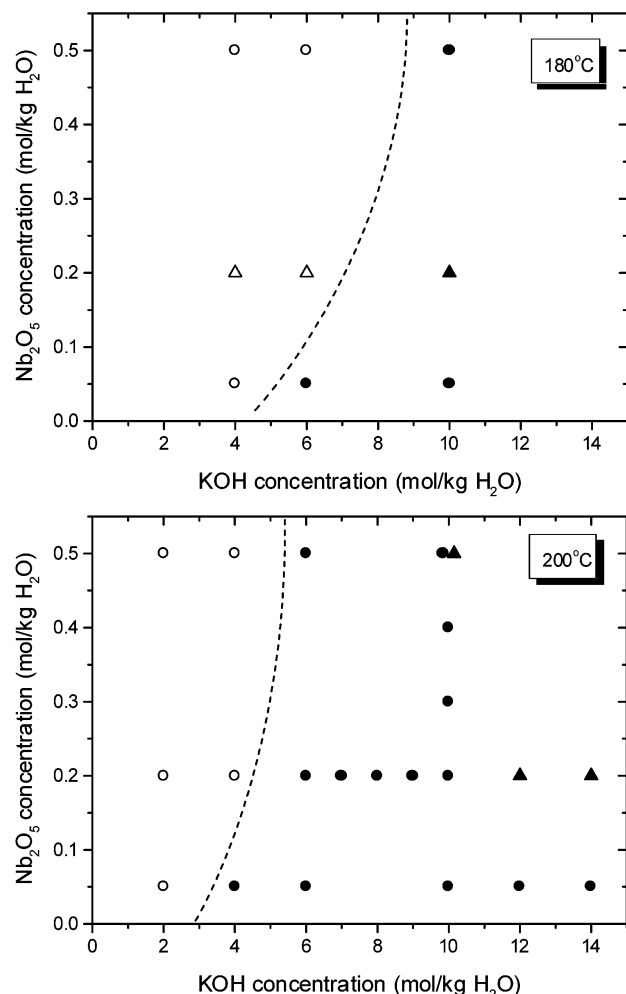


Figure 8. Maps showing deposition of KNbO₃ films under hydrothermal conditions at 180 and 200 °C for 48 h: open symbols denote no film formation; solid symbols denote formation of KNbO₃ films; circles represent deposition (or attempted deposition) of orthorhombic KNbO₃ films on SrTiO₃ (100) substrates, and triangles represent deposition (or attempted deposition) of KNbO₃ films on LiTaO₃ (001).

concentration. Single crystal-like orthorhombic KNbO₃ films with (011) orientation and 45 nm to 1.28 μm thickness were formed at KOH concentrations of 4.0–6.0 m, almost irrespectively of the Nb₂O₅ concentration. The (011) orientation with respect to the (100) orientation of the SrTiO₃ substrate was already observed in other works.⁵⁰ Single crystallographic orientation of the KNbO₃ films in conjunction with the low synthesis temperature may indicate single-domain nature of the films. However, existence of domains in the KNbO₃ film cannot be easily distinguished by XRD.⁵⁰ The morphology of these films resembled layered growth of nm-size clusters forming dendritic/fractal-like microstructures. Similar microstructures were observed earlier in the case of epitaxial Pb(Zr_xTi_{1-x})O₃ (PZT) films deposited under hydrothermal conditions.⁴⁶ This kind of microstructure is typical for growth of single crystals from molecular clusters⁵¹ strongly suggesting single-crystal nature of the epitaxial KNbO₃ (011) films. At the KOH concentrations of 7.0 m and higher, the KNbO₃ films

exhibited mixed (100)/(011) orientation. With increasing concentrations of both reactants, the films were initially covered with islands and subsequently with uniform and very thick layers of strongly textured orthorhombic KNbO₃. The mixed crystallographic orientation appears to be associated with the thickest films, i.e., >3.5 μm, and could be ascribed to multidomain formation as a relaxation mechanism of thermoelastic stresses, which increase within the film with increasing thickness.⁵²

The described hydrothermal synthesis of epitaxial orthorhombic KNbO₃ films has the following advantages as compared to the previously used techniques. The deposition technique utilizes low-temperature aqueous solutions and simple reactants (Nb₂O₅ powder, KOH). Because the synthesis can be accomplished below the orthorhombic–tetragonal phase transition temperature of 225 °C, orthorhombic KNbO₃ films with a single crystallographic orientation, and probably also single-domain structure, can be formed in a well-defined range of synthesis conditions, which have been established for the first time in this work. The films can be uniformly distributed on the entire substrate area without stirring, exhibit high stoichiometry, and do not show evidence of interdiffusion or chemical reaction at the film/substrate interface, which is often associated with the high-temperature processing. In addition, the KNbO₃ is a lead-free material, which, together with excellent piezoelectric and optical properties of the KNbO₃ film, implies many optical, surface acoustic wave, and other applications.

Hydrothermal deposition of KNbO₃ films is, of course, not limited to substrates such as SrTiO₃ and LiTaO₃. Capability of the hydrothermal method to deposit films with different orientations, morphologies, and chemical compositions on various substrates has been demonstrated in many works.^{42,53,54} It is also worth mentioning that KNbO₃ is known to form a variety of solid solutions, for example (Na,K)NbO₃,⁵⁵ (Li,K)NbO₃,⁵⁶ K(Nb,Ta)O₃,³² (K_{0.5}Bi_{0.5})TiO₃–KNbO₃,⁵⁷ BaTiO₃–KNbO₃,⁵⁸ and PZN–KNbO₃–PZT,⁵⁹ etc. KNbO₃ can be also doped with a variety of ions, such as Li⁺, Ba²⁺, Sm³⁺, Ce⁴⁺, and V⁵⁺, etc.⁶⁰ All these materials exhibit a variety of attractive piezoelectric, ferroelectric, and electrooptic properties, which can be tailored by properly adjusting their chemical compositions. Most important among the principal features of the hydrothermal synthesis is that it allows an easy synthesis of a variety of solid solutions in the form of films. Good examples are PZT films⁴² or (Ba,Ca,Sr)(Mo,W)O₃ films.⁶¹ Therefore, the results of the present work strongly imply the possibility of hydrothermal deposition of thin films of a variety of solid-solution compositions based on KNbO₃, particularly

(52) Ohring, M. *The Materials Science of Thin Films*; Academic Press: New York, 1992.

(53) Yoshimura, M.; Suchanek, W. *Solid State Ionics* **1997**, *98*, 197.

(54) Suchanek, W. L.; Yoshimura, M. *J. Am. Ceram. Soc.* **1998**, *81*, 2864.

(55) Egerton, L.; Dillon, D. M. *J. Am. Ceram. Soc.* **1959**, *42*, 438.

(56) Zhang, H. X.; Kam, C. H.; Zhou, Y.; Han, X. Q.; Cheng, S. D.; Chan, C. Y.; Lam, Y. L. *J. Mater. Res.* **2001**, *16*, 3609.

(57) Wada, T.; Toyoiike, K.; Imanaka, Y.; Matsuo, Y. *Jpn. J. Appl. Phys., Part 1* **2001**, *40*, 5703.

(58) Ravez, J.; Simon, A. *Solid State Sci.* **1999**, *1*, 25.

(59) Takenaka, T.; Satou, M.; Nakata, K.; Sakata, K. *Ferroelectrics* **1992**, *128*, 67.

(60) Ding, S.; Shen, J. *J. Am. Ceram. Soc.* **1990**, *73*, 1449.

(61) Cho, W.-S.; Yoshimura, M. *J. Appl. Phys.* **1998**, *83*, 518.

(50) Gopalan, V.; Raj, R. *J. Am. Ceram. Soc.* **1996**, *79*, 3289.

(51) Askhabov, A. M. *Sytkytkar Mineralogical Collection* **2001**, *30*, 14.

because many of the materials mentioned above can be synthesized under mild hydrothermal conditions.

Conclusions

KNbO₃ thin films were deposited on single-crystal oxide substrates, including 1-in. wafers, by hydrothermal epitaxy at 180–210 °C using simple reactants. Well-defined ranges of synthesis conditions for the KNbO₃ films in terms of temperatures and reactants concentrations were established. The KNbO₃ films with 45 nm to 3.5 μm thickness were uniformly distributed on the entire substrate area without stirring, exhibited high stoichiometry, and did not show evidence of interdiffusion or chemical reaction at the film/substrate interface. Neither cracks nor peeling-off were observed in most cases. High levels of crystallographic orientation and microstructures of some of the films suggest single-

crystal growth. The low synthesis temperatures, which are below the 225 °C phase transition temperature of KNbO₃, allowed synthesis of pure orthorhombic epitaxial KNbO₃ films with (011) orientation and probably single-domain that are expected to exhibit improved properties as compared to the films prepared by high-temperature processing.

Acknowledgment. I thank Gary Johnson, Paul Hervey, Mark Polster, and Vladimir Klipov (Sawyer Research Products) for discussions, Paul Lawson and Brian Dezman (Sawyer) for managing the autoclave operations, John Sears (Case Western Reserve University) for SEM observations, and Alan McIlwain (Case) for introducing the XRD system and conducting the RBS measurements.

CM034952Q